Toxicology and Applied Pharmacology 270 (2013) 31–38

Contents lists available at SciVerse ScienceDirect

Toxicology and Applied Pharmacology

journal homepage: www.elsevier.com/locate/ytaap

Reactive oxygen species produced by NADPH oxidase and mitochondrial dysfunction in lung after an acute exposure to Residual Oil Fly Ashes

Natalia D. Magnani [a], Timoteo Marchini [a], Virginia Vanasco [a], Deborah R. Tasat [b], Silvia Alvarez [a], Pablo Evelson [a,*]

[a] Instituto de Bioquímica Medicina Molecular (IBIMOL-UBA-CONICET), Facultad de Farmacia y Bioquímica, Universidad de Buenos Aires, Buenos Aires, Argentina
[b] CESyMA, Escuela de Ciencia y Tecnología, Universidad Nacional de San Martín, San Martín, Buenos Aires, Argentina

ARTICLE INFO

Article history:
Received 18 January 2013
Revised 28 March 2013
Accepted 1 April 2013
Available online 10 April 2013

Keywords:
Air pollution
Lung
Mitochondria
NADPH oxidase
Residual oil fly ash (ROFA)
Reactive O_2 species

ABSTRACT

Reactive O_2 species production triggered by particulate matter (PM) exposure is able to initiate oxidative damage mechanisms, which are postulated as responsible for increased morbidity along with the aggravation of respiratory diseases. The aim of this work was to quantitatively analyse the major sources of reactive O_2 species involved in lung O_2 metabolism after an acute exposure to Residual Oil Fly Ashes (ROFAs). Mice were intranasally instilled with a ROFA suspension (1.0 mg/kg body weight), and lung samples were analysed 1 h after instillation. Tissue O_2 consumption and NADPH oxidase (Nox) activity were evaluated in tissue homogenates. Mitochondrial respiration, respiratory chain complexes activity, H_2O_2 and ATP production rates, mitochondrial membrane potential and oxidative damage markers were assessed in isolated mitochondria. ROFA exposure was found to be associated with 61% increased tissue O_2 consumption, a 30% increase in Nox activity, a 33% increased state 3 mitochondrial O_2 consumption and a mitochondrial complex II activity increased by 25%. During mitochondrial active respiration, mitochondrial depolarization and a 53% decreased ATP production rate were observed. Neither changes in H_2O_2 production rate, nor oxidative damage in isolated mitochondria were observed after the instillation. After an acute ROFA exposure, increased tissue O_2 consumption may account for an augmented Nox activity, causing an increased $O_2^{\bullet-}$ production. The mitochondrial function modifications found may prevent oxidative damage within the organelle. These findings provide new insights to the understanding of the mechanisms involving reactive O_2 species production in the lung triggered by ROFA exposure.

Introduction

Epidemiological studies have established a direct correlation between increased environmental air particulate matter (PM) levels and adverse health effects, resulting in increased morbidity and mortality rates due to cardiopulmonary diseases (Dominici et al., 2006). This association was observed not only for long term exposures to PM, but also for acute exposures, where variations in health end points and the occurrence of lower respiratory diseases, cough and asthma exacerbation have been reported (Pope, 2000). Moreover, individuals with preexistent heart and lung diseases are at particularly high risk after an air pollution episode (Ostachuk et al., 2008).

Airborne PM is comprised of a mixture of solid and liquid particles emitted into the atmosphere from natural sources, such as forest fires, volcanic emissions and sea spray; and from anthropogenic sources including vehicle exhaust, fossil fuel combustion during power generation and industrial processes, smelting and mining (Nel, 2005). Among this last category, residual oil fly ash (ROFA) results from an incomplete combustion of carbonaceous materials and significantly contribute to ambient air PM burden (Costa and Dreher, 1997). Given that it is especially rich in transition metals (namely iron, nickel and vanadium), ROFA is the most frequently PM surrogate used in order to evaluate their role in the oxidative metabolism alterations, which leads to lung damage (Ghio et al., 2002).

Lung injury after air pollution inhalations has been suggested to be triggered by local reactive O_2 species production which, in turn, could be generated not only from the particles themselves, but also from the chemicals coated on their surface. Moreover, O_2-derived free radicals may also be generated by the interaction of particle pollutants and their components, with cellular enzymes and organelles (Li et al., 2008).

The reactive O_2 species burden elicited by several environmental agents leads to an airway inflammatory response, which includes

Abbreviations: PM, particulate matter; ROFAs, Residual Oil Fly Ashes; $O_2^{\bullet-}$, superoxide anion; Nox, NADPH oxidase; RCR, respiratory control ratio; m-CCCP, carbonyl cyanide m-chlorophenylhydrazone; $\Delta\Psi_m$, mitochondrial membrane potential; $DiOC_6$, 3,3′-dihexyloxacarbocyanine iodide; NAO, 10-*N*-nonyl acridine orange; TBARS, thiobarbituric acid reactive substances.

* Corresponding author at: Institute of Biochemistry and Molecular Medicine (IBIMOL-CONICET), School of Pharmacy and Biochemistry, University of Buenos Aires, Junín 956 (1113), Buenos Aires, Argentina.
E-mail address: pevelson@ffyb.uba.ar (P. Evelson).

0041-008X/$ – see front matter © 2013 Elsevier Inc. All rights reserved.
http://dx.doi.org/10.1016/j.taap.2013.04.002

leukocyte recruitment, activation and increased alveolar macrophage count (Becker et al., 2002). Interestingly, activated phagocytic cells after ROFA exposure produce reactive O_2 species through the assembly and activation of the Nox complex (Magnani et al., 2011). The primary role of this complex in its active form is to catalyse transmembrane transfer of electrons from cytosolic NADPH to molecular O_2 within the extracellular space or specialized cell compartments. This reaction leads to $O_2^{\bullet-}$ production, that may subsequently dismutate to hydrogen peroxide (H_2O_2), which is able not only to diffuse through biological membranes and function as a host defence, but also to regulate intracellular signalling pathways (van der Vliet, 2008).

It is well established that mitochondria represent an important modulator of the cellular response to a wide variety of metabolic and environmental stressors. Moreover, $O_2^{\bullet-}$ is also produced by this organelle under normal physiological conditions as a by-product of redox reactions during electron transport in the respiratory chain (Andreyev et al., 2005). An imbalance in oxidants production can trigger intracellular signalling cascades causing oxidative damage to cellular and mitochondrial macromolecules, which have been associated with the development of respiratory diseases, such as chronic obstructive pulmonary diseases (COPD) (Aguilera-Aguirre et al., 2009). In addition to serving as an oxidant production source, mitochondria are highly susceptible to reactive O_2 species, which could also indirectly perturb the organelle function (Xia et al., 2007).

Considering that lung injury mediated by reactive O_2 species appears to be a key mechanism in the observed damage triggered by exposure to ambient pollutants, the aim of this work was to analyse the mechanisms of reactive O_2 species production sources involved in lung oxidative damage after an acute exposure to ROFA particles.

Materials and methods

Drugs and chemicals. All chemicals were purchased from Sigma-Aldrich Chemical Company (St Louis, MO, USA), except for HCl, H_2SO_4, and organic solvents which were purchased from Merck KGaA (Darmstadt, Germany). The gp91 ds-tat peptide was provided by AnaSpec (Fremont, CA, USA). NAO and $DiOC_6$ were purchased from Molecular Probes.

Experimental model. *ROFA suspension.* Residual oil fly ash (ROFA) was employed as a recognized ambient PM and was generously provided by J. Godleski (Harvard School of Public Health, Boston, MA, USA). It was collected in Boston Edison Co., Mystic Power, plant number 4, CT, USA (Killingsworth et al., 1997). ROFA samples from this source have been previously characterized in terms of elemental composition and particle size. Vanadium, nickel and iron are the predominant metals present as water-soluble sulphates, and particle mean aerodynamic diameter is 2.06 ± 1.57 μm (Martin et al., 2007; Ostachuk et al., 2008). PM suspension was freshly prepared by resuspending ROFA particles in sterile saline solution at a final concentration of 0.5 mg/ml, followed by 10 min incubation in an ultrasonic water bath (Goldsmith et al., 1998).

Animal exposure. Female Swiss mice weighing 20–25 g were exposed to ROFA particles by the nasal drop technique as previously described (Southam et al., 2002). Briefly, mice were lightly anaesthetized (ip) with 1 ml/kg body weight of xylazine (2%) and ketamine (50 mg/ml), and intranasally instilled with 50 μl of the ROFA suspension (1.0 mg/kg body weight) delivered in a single dose. Control mice were instilled with 50 μl of the vehicle. The selection of the ROFA dose was based on results shown in previous studies (Arantes-Costa et al., 2008; Magnani et al., 2011). Animals were euthanized 1 h after the exposure with an anaesthesia overdose, and lung samples were collected. Animal treatment was carried out in accordance with the guidelines of the 6344/96 regulation of the Argentinean National Drug, Food and Medical Technology Administration (ANMAT).

Nox inhibitor administration. The gp91 ds-tat peptide was dissolved in sterile saline solution and administrated (ip) (10 mg/kg body weight) 30 min before the ROFA exposure (Rey et al., 2001).

Samples preparation. *Tissue cubes.* Once the exposure time was reached, animals were euthanized and lungs were removed and immediately placed in ice-cold Krebs buffer solution [118 mM NaCl, 4.7 mM KCl, 1.2 mM KH_2PO_4, 1.2 mM $MgSO_4$, 2.5 mM $CaCl_2$, 24.8 mM $NaHCO_3$ and 5.5 mM glucose (pH 7.4)]. After being washed and weighted, 1 mm^3 tissue cubes were cut by the use of a scalpel (Vanasco et al., 2008).

Tissue homogenates. Lung samples (0.2 g of wet weight) were homogenized with a glass-Teflon homogenizer in a medium consisting of 120 mM KCl, 30 mM phosphate buffer (pH 7.4) (1:5) at 0–4 °C. The suspension was centrifuged at 600 *g* for 10 min at 4 °C to remove nuclei and cell debris. The pellet was discarded and the supernatant was used as "homogenate" (Evelson et al., 2001).

Mitochondrial isolation. Lung mitochondrial purified fractions were obtained from tissue homogenates by differential centrifugation. Tissues samples were homogenized in a medium consisting of 0.23 M mannitol, 0.07 M sucrose, 10 mM Tris–HCl, and 1 mM EDTA (pH 7.4). Samples were centrifuged at 700 *g* for 10 min to discard nuclei and cell debris. The sediment was discarded and the supernatant was centrifuged at 8000 *g* for 10 min to obtain the enriched mitochondria fraction. The mitochondrial pellet was washed twice and resuspended in a minimum volume of the same buffer. The whole procedure was carried out at 0–4 °C. Purity of isolated mitochondria was assessed by determining lactate dehydrogenase activity; only mitochondria with less than 3% of cytosolic lactate dehydrogenase activity were used (Cadenas and Boveris, 1980).

Mitochondrial membranes. Mitochondrial membranes were obtained by three freeze–thaw cycles of the mitochondrial preparation, followed by a homogenization step by passage through a 29G hypodermic needle (Mela and Seitz, 1979).

Oxygen consumption by tissue cubes. A two-channel respirometer for high-resolution respirometry (Hansatech Oxygraph, Hansatech Instruments Ltd., Norfolk, England) was used. Briefly, O_2 consumption rates were measured at 30 °C in a respiration medium containing 118 mM NaCl, 5 mM KCl, 1.2 mM KH_2PO_4, 1.2 mM $MgSO_4$, 2.5 mM $CaCl_2$, 25 mM $NaHCO_3$ and 5.5 mM glucose (pH 7.4) (Poderoso et al., 1994). KCN (4 mM) was added to the reaction chamber as a mitochondrial cytochrome oxidase inhibitor (Vanasco et al., 2012). Results were expressed as ng-at O/min g tissue.

Nox activity. *Lucigenin Chemiluminescence (LCL).* The Lucigenin-derived chemiluminescence method was used as an indirect measurement of Nox activity (Vaquero et al., 2004). Briefly, 50 μg of protein tissue homogenate was diluted in 250 μl of 50 mM phosphate buffer containing 1 mM EGTA and 150 mM sucrose (pH 7.4). Lucigenin (50 μM) was added to the reaction media, 100 μM NADPH was used as substrate, and chemiluminescence was immediately measured at 15 s intervals for 3 min in a Labsystems Luminoskan RS Microplate Reader (Labsystem, Ramsey, Minnesota). The specificity of the assay was confirmed by the addition of superoxide dismutase (200 U/ml) as an $O_2^{\bullet-}$ scavenger. Results were expressed in arbitrary units (AU)/mg prot.

NADPH consumption rate. Tissue homogenate (50 μg prot.) was diluted in 2 ml 100 μM phosphate buffer (pH 7.4) and incubated with 100 μM NADPH at 37 °C. NADPH consumption rate was followed

spectrophotometrically at 340 nm during 30 min (Wei et al., 2006). Results were expressed as nmol NADPH/min mg prot.

Mitochondrial respiration. Mitochondrial O_2 consumption was followed polarographically with a Clark-type O_2 electrode (Hansatech Oxygraph, Hansatech Instruments Ltd, Norfolk, England) for high resolution respirometry. Mitochondrial respiratory rates were measured in a reaction medium containing 0.23 M mannitol, 0.07 M sucrose, 20 mM Tris–HCl, 1 mM EDTA, 4 mM $MgCl_2$, and 5 mM phosphate (pH 7.4) at 30 °C. Succinate (8 mM) was used as substrate to establish state 4 (resting or controlled respiration), while state 3 (active respiration) was triggered by the addition of 0.5 mM ADP. Respiratory control ratio (RCR) was calculated as the ratio between state 3 and state 4 respiration rates. Results were expressed as ng-at O/min mg prot. (Boveris et al., 1999). Oligomycin (2 μM) was used as a F_o–F_1 ATP synthase inhibitor to reach $4_{Oligomycin}$ (state 4_O) respiration. Afterwards, the protonophore carbonyl cyanide m-chlorophenylhydrazone (m-CCCP) (2 μM) was added to evaluate mitochondrial uncoupled respiration (state 3_U) (Brand and Nicholls, 2011).

Mitochondrial respiratory chain complexes activity. NADH-cytochrome c reductase activity (complexes I–III). Mitochondrial respiratory complexes I–III activity was evaluated by a colorimetric assay following cytochrome c^{3+} reduction rate at 550 nm ($\varepsilon = 19\ mM^{-1}\ cm^{-1}$) and 30 °C. Mitochondrial membranes (1.0 mg prot./ml) were added to 100 mM phosphate buffer (pH 7.2), supplemented with 0.2 mM NADH, 25 μM cytochrome c^{3+} and 0.5 mM KCN. Results were expressed as nmol reduced cytochrome c^{3+}/min mg prot.

Succinate cytochrome c reductase activity (complexes II–III). Succinate cytochrome *c* reductase activity (complexes II–III) was determined by a colorimetric assay following cytochrome c^{3+} reduction rate at 550 nm ($\varepsilon = 19\ mM^{-1}\ cm^{-1}$) and 30 °C. Mitochondrial membranes (1.0 mg prot./ml) were added to 100 mM phosphate buffer (pH 7.2), supplemented with 5 mM succinate, 25 μM cytochrome c^{3+} and 0.5 mM KCN. Results were expressed as nmol reduced cytochrome c^{3+}/min mg prot.

Cytochrome oxidase activity (complex IV). Cytochrome oxidase activity (complex IV) was assayed spectrophotometrically by following the decrease in absorbance due to cytochrome c^{2+} oxidation at 550 nm ($\varepsilon = 19\ mM^{-1}\ cm^{-1}$) and 30 °C. As cytochrome c^{2+} oxidation has a pseudo-first order kinetics, complex IV activity was calculated from the kinetic constant (k'). Mitochondrial membranes (1.0 mg prot./ml) were incubated at 30 °C in 100 mM phosphate buffer (pH 7.2) supplemented with 60 μM cytochrome c^{2+}. Results were expressed as k'/mg prot. Cytochrome c^{2+} was freshly prepared by reduction of cytochrome c^{3+} with sodium dithionite, and separated from the reducing agent by exclusion chromatography in a Sephadex-G25 column (Yonetani, 1967).

ATP production rate. A chemiluminescence assay based on the luciferin–luciferase system was used. Mitochondrial ATP production rate was determined in freshly purified mitochondria incubated in respiration buffer consisting of 150 mM KCl, 25 mM Tris–HCl, 2 mM EDTA, 0.1% (w/v) BSA, 50 mM PBS and 100 μM $MgCl_2$ (pH 7,4), supplemented with 40 μM D-luciferin, 0.05 μg/ml luciferase and 150 μM di(adenosine) pentaphosphate, used in order to inhibit adenylate kinase, thus increasing assay specificity. ATP production was triggered by the addition of 8 mM succinate and 125 mM ADP to the reaction well (Drew and Leeuwenburgh, 2003). Measurements were carried out at 30 °C in a Labsystems Luminoskan RS Microplate Reader (Labsystem, Ramsey, Minnesota, USA). A negative control with 2 μM oligomycin was included in order to confirm that the emitted chemiluminescence is due to ATP synthesis by the F_o–F_1 ATP synthase. A calibration curve was performed using ATP as standard. Results were expressed as nmol ATP/min mg prot. In order to evaluate the efficiency of the oxidative phosphorylation process, the number of phosphorylated ADP molecules per oxygen atom (P/O ratio) was calculated as ATP production/state 3 O_2 consumption rates.

Mitochondrial membrane potential ($\Delta\Psi_m$). Freshly isolated lung mitochondria (100 μg prot./ml) were incubated with the potentiometric cationic probe 3,3′-dihexyloxacarbocyanine iodide ($DiOC_6$) (30 nM) in respiration buffer. The procedure was performed in the dark at 37 °C for 20 min. After the incubation period, mitochondria were acquired by a Partec PAS-III flow cytometer (Partec GmbH, Münster, Germany) equipped with a 488 nm argon laser. To exclude debris, samples were gated based on light-scattering properties and 30,000 events per sample within this gate (R1) were collected. 10-N-nonyl acridine orange (NAO) (100 nM) was used to selectively stain mitochondria and evaluate the purity of the mitochondrial preparations. In order to quantify the resulting changes in membrane potential after the addition of 8 mM succinate (state 4) and 125 mM ADP (state 3) to the reaction mixture, $DiOC_6$ signal was analysed in the FL-1 channel and the arithmetic mean values of the median fluorescence intensities (MFI) were obtained. Total depolarization induced by 2 μM m-CCCP was used as a positive control. Mitochondrial preparations that showed no changes in membrane potential under this condition were discarded (Czerniczyniec et al., 2011).

H_2O_2 production rate. Mitochondrial H_2O_2 production rate was assessed by the scopoletin–horseradish peroxidase (HRP) method, following the decrease in fluorescence intensity at 365–450 nm (λ_{exc}–λ_{em}) and 30 °C (Boveris, 1984). Lung mitochondrial purified fractions were added to the reaction medium consisting of 0.23 mM mannitol, 0.07 M sucrose, 20 mM Tris–HCl, 2500 U/ml HRP, 0.6 mM scopoletin, and 15,000 U/ml superoxide dismutase (pH 7.4). H_2O_2 production was triggered by the addition of 8 mM succinate. A calibration curve was performed with H_2O_2 solutions (ranging from 0.05 to 0.35 mM). Results were expressed as nmol H_2O_2/min mg prot.

Oxidative damage markers. Thiobarbituric acid reactive substances (TBARS) assay. Oxidative damage to phospholipids was evaluated as TBARS by a fluorometric assay (Yagi, 1976). Briefly, 100 μl of isolated mitochondrial suspensions were added to 200 μl 0.1 N HCl, 30 μl 10% (w/v) phosphotungstic acid and 100 μl 0.7% (w/v) 2-thiobarbituric acid. The mixture was heated in boiling water for 60 min. TBARS were extracted in 1 ml of *n*-butanol. After a centrifugation at 1000 *g* for 10 min, the fluorescence of the butanolic layer was measured in a Perkin Elmer LS 55 luminiscence spectrometer at 515 nm (excitation) and 553 nm (emission). A calibration curve was prepared using 1,1,3,3-tetramethoxypropane as standard. Results were expressed as pmol TBARS/mg prot.

Determination of carbonyl content. The content of carbonyl groups in oxidative modified mitochondrial proteins was measured by the amount of 2,4-dinitrophenilhydrazone formed upon reaction with 2,4-dinitrofenilhydrazine (DNPH) (Levine et al., 1994). Isolated mitochondria were incubated with 2 mM DNPH at room temperature for 1 h in the dark and vortexed every 15 min. Proteins were precipitated with 20% (w/v) TCA, incubated on ice for 10 min and centrifuged at 10,000 *g* for 10 min at 4 °C. The supernatant was discarded and the previous procedure was repeated with 10% (w/v) TCA. The pellet was washed with 1 ml ethanol:ethyl acetate (1:1) and centrifuged at 10,000 *g* for 10 min at 4 °C. This procedure was repeated 3 times. Finally, the pellet was resuspended in 6 M guanidine hydrochloride (pH 2.5) and incubated at 37 °C for 10 min. Carbonyl content was calculated from the absorbance at 360 nm ($\varepsilon_{390-350} = 22\ mM^{-1}\ cm^{-1}$). Results were expressed as nmol carbonyl groups/mg prot.

Protein content. Protein concentration was measured by the method of Lowry et al. (1951) using bovine serum albumin as standard.

Statistics. Results were expressed as mean value ± SEM and represent the mean of at least six independent experiments. The number of independent experiments reflects the number of animals used for each assay. Unpaired Student's *t*-test for unpaired data was used to analyse differences between mean values of two groups. ANOVA followed by Tukey test was used to analyse differences between mean values of more than two groups. Statistical significance was considered at $p < 0.05$.

Results

Oxygen consumption by tissue cubes

To evaluate O_2 consumption by the whole tissue, respiration rates were assessed in 1 mm^3 lung tissue cubes, a thickness which allows O_2 diffusion to the centre of the cube, avoiding anaerobic areas (Valdez et al., 2011). As it is shown in Table 1, a 55% increase was observed after the ROFA exposure when compared with the control group. Animals pretreated with the Nox inhibitor, gp91 ds-tat, showed a significant decrease (30%) in O_2 consumption, when compared with the ROFA-exposed group. However, a slight but significant increase in lung O_2 consumption (9%) was still present in ROFA-exposed animals, which were pretreated with gp91 ds-tat when compared with the control group.

The analysis of O_2 uptake by non-mitochondrial sources was carried out by measuring tissue O_2 consumption in presence of 4 mM KCN. Representative traces are shown in Fig. 1. After ROFA instillation, a significant difference between the ROFA and control group was still present (27%) in this condition, which was abolished by gp91 ds-tat pretreatment (Table 1). The remaining O_2 consumption in the ROFA group after the inhibition of both main O_2 consumption sources, which may account for non-mitochondrial sources other than Nox, showed no significant differences with the values from control animals.

In order to clarify the mechanisms underlying these phenomena, the relative contribution of the main free radical sources was studied. Using this approach, the determination of Nox activity and mitochondrial O_2 consumption was carried out.

Nox activity in lung homogenates

Nox plays a key role as a source of reactive O_2 species under inflammatory conditions. Nox activity was evaluated through two different assays in lung homogenates: by the lucigenin chemiluminescent (LCL) probe, and spectrophotometric determination of NADPH consumption rate. Results are shown in Fig. 2. A similar significant increase was found for the ROFA group in both assays, in comparison with control animals. LCL showed a 26% increase (control: 0.66 ± 0.02 UA/mg prot.; $p < 0.0001$), while a 31% increase in NADPH consumption rate was observed (control: 0.74 ± 0.01 μmol NADPH/min. mg prot.; $p < 0.0001$).

In order to test the specificity of both assays, animals were pretreated with the NADPH oxidase inhibitor gp91 ds-tat. As it is shown in Fig. 2, the ROFA + gp-91 ds tat group showed a significant decrease when compared to ROFA (35% in NADPH consumption and 25% LCL), indicating that the observed increase in LCL and NADPH consumption rate after ROFA exposure was abolished by pretreatment with the Nox inhibitor.

Table 1
Oxygen consumption by tissue cubes in lung after exposure to ROFA in the presence or absence of KCN 4 mM and gp91 ds-tat. Data is presented as mean ± SEM, n = 6.

	Control	ROFA	ROFA + gp91 ds tat
Oxygen consumption (ng-at O/min g tissue)	228 ± 7	354 ± 8*	249 ± 13*#
Oxygen consumption + KCN (ng-at O/min g tissue)	48 ± 2	61 ± 2*	38 ± 5#

*$p < 0.001$ vs control group, #$p < 0.001$ vs ROFA (unpaired *t*-test).

Oxygen consumption by lung mitochondria

O_2 consumption by isolated mitochondria in state 4 and 3 were measured and the corresponding RCR were calculated. As it is shown in Table 2, the exposure to ROFA significantly increased mitochondrial state 3 O_2 consumption by 34%, while no significant changes were observed in state 4. When state 4_O respiration was reached by the addition of 2 μM oligomycin into the reaction chamber, no significant differences in O_2 consumption were observed between both groups. Moreover, in ROFA-exposed mice, no differences were observed in mitochondrial O_2 uptake in state 3_U after the addition of 2 μM m-CCCP (Table 2).

Mitochondrial respiratory chain complexes activity

Taking into account the observed changes in lung mitochondrial active respiration after ROFA exposure, mitochondrial respiratory chain complex activities were evaluated. Mitochondrial respiratory chain complex II activity was found to be significantly increased by 25% in ROFA-exposed mice, whereas no statistical differences in complexes I and IV activities were found in ROFA-exposed mice when compared with the control group. Results are shown in Table 3.

Mitochondrial ATP production rate

Mitochondria, through a highly efficient process, convert chemical energy derived from O_2 reduction to water into the proton-motive force used to drive the endergonic synthesis of ATP. A chemiluminescence assay based on the luciferin–luciferase system was used to determine mitochondrial ATP production rate. A 33% significant decrease was found after ROFA inhalation (control: 330 ± 30 nmol/min mg prot., $p < 0.05$) (Fig. 3).

P/O ratio

Considering mitochondrial state 3 O_2 consumption and mitochondrial ATP production rates, the number of phosphorylated ADP molecules per O_2 atom (P/O ratio) was calculated (Brand and Nicholls 2011). While a value of 3.2 was obtained for the control group, the P/O ratio in PM-exposed mice was 1.5.

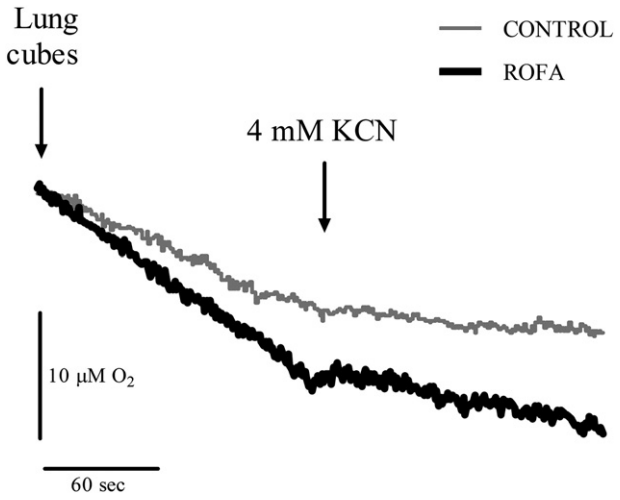

Fig. 1. Representative traces obtained during the measurement of lung tissue cubes O_2 consumption rates before and after the addition of 4 mM KCN.

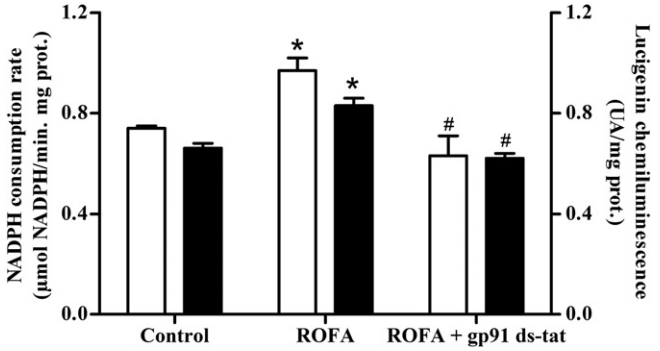

Fig. 2. Nox activity assayed by the spectrophotometric determination of NADPH consumption rate (□) and the measurement of $O_2^{\bullet-}$ production, using the lucigenin chemiluminescence probe (■) after exposure to ROFA. Data is presented as mean ± SEM, n = 6. *$p < 0.05$ vs. control and #$p < 0.01$ vs. ROFA (ANOVA followed by Tukey test).

Mitochondrial membrane potential ($\Delta\Psi_m$)

Mitochondrial membrane potential represents another key mitochondrial function parameter. To assess $\Delta\Psi_m$, mitochondria were selected by light-scattering properties (Fig. 4A) and the fluorescence after incubation with NAO, which selectively binds to cardiolipin in the inner mitochondrial membrane (Fig. 4B). As presented in overlayed $DiOC_6$ fluorescence histograms (Fig. 4C) and quantification of $DiOC_6$ fluorescence (Fig. 4D), ROFA values remained unchanged compared with the control group when $\Delta\Psi_m$ was evaluated during mitochondrial resting respiration (control: 60 ± 3 AU). However, when active respiration was established, ROFA $\Delta\Psi_m$ was found to be 12% lower than control $\Delta\Psi_m$ (control: 50 ± 2 AU; $p < 0.05$), which indicates a significant depolarization in isolated mitochondria from ROFA-instilled mice.

Mitochondrial H_2O_2 production rate

The observed increased in state 3 respiration rate after PM exposure could lead to the production of oxidant species which enhance cellular oxidative damage. Mitochondrial H_2O_2 production rate by lung mitochondria was measured and the results are shown in Fig. 5. No significant differences were observed between both experimental groups (control: 2.50 ± 0.50 nmol/min mg prot.; ROFA: 2.20 ± 0.40 nmol/min mg prot.).

Mitochondrial oxidative damage markers

TBARS levels and protein carbonyl content are well-established direct markers of oxidative damage to lipids and proteins, respectively. TBARS and carbonyl content levels of isolated lung mitochondria were determined. No significant changes were observed in either lipid (control: 1200 ± 80 pmol TBARS/mg prot.; ROFA: 1100 ± 100 pmol TBARS/mg prot.) or protein oxidative markers (control: 1.7 ± 0.2 nmol/mg prot.; ROFA: 1.7 ± 0.2 nmol/mg prot.) (Fig. 6).

Table 2
Oxygen consumption and respiratory control of mitochondria isolated from lung of mice exposed to ROFA. Data is presented as mean ± SEM, n = 6.

	Control	ROFA
State 3 (ng-at O/min mg prot.)	103 ± 5	138 ± 5[a]
State 4 (ng-at O/min mg prot.)	52 ± 2	54 ± 2
RCR	2.0	2.7
State 3_U (ng-at O/min mg prot.)	127 ± 9	140 ± 10
State 4_O (ng-at O/min mg prot.)	52 ± 2	62 ± 4

[a] $p < 0.001$ vs control group (unpaired *t*-test).

Table 3
Mitochondrial respiratory complex activity from lung of mice exposed to ROFA. Data is presented as mean ± SEM, n = 6.

	Control	ROFA
Complexes I–III (nmol/min mg prot.)	220 ± 10	230 ± 10
Complexes II–III (nmol/min mg prot.)	14 ± 1	18 ± 1[a]
Complex IV ($k'10^{-2}$/min mg prot.)	250 ± 40	250 ± 40

[a] $p < 0.005$ vs control group (unpaired *t*-test).

Discussion

It is accepted that exposure to air pollution PM triggers within the lung an inflammatory response, endothelial activation and oxidative stress (Chen and Lippmann, 2009). In this scenario, the analysis of lung O_2 metabolism appears to be an important area of study with the aim of understanding free radicals production mechanisms, which may lead to the onset or aggravation of respiratory diseases.

Lung tissue O_2 consumption was found to be significantly increased by 55% after the exposure to ROFA particles. Several mechanisms have been suggested to explain the observed raise, such as increased enzymatic activities and changes in mitochondrial respiration (Vanasco et al., 2008). Two different approaches were used to deeply analyse O_2 consumption after the exposure to ROFA particles: a) pretreatment with the Nox inhibitor gp91 ds-tat and, b) measurements in the presence of 4 mM KCN. Pretreatment with gp91 ds-tat was used to establish the relative contribution of Nox to the observed increase in tissue O_2 consumption. It is well known that the activation of Nox is triggered via protein kinase C (PKC)-mediated phosphorylation of cytosolic p47phox, which then binds to membrane-associated gp91phox (Bedard and Krause, 2007). The gp91 ds-tat peptide inhibits the interaction between gp91phox and p47phox, necessary for the full activation of the enzyme (Rey et al., 2001). Results obtained when animals were previously injected with gp91 ds-tat showed that Nox is an important source of the observed raise in O_2 consumption.

Nox is of particular interest as an important non-mitochondrial source of reactive O_2 species elicited by airway inflammation (van der Vliet, 2011). It has been shown that environmental particles, when internalized by phagocytosis after inhalation, trigger an increased alveolar macrophage count (Becker et al., 2002). Taking into account that Nox2 is expressed in macrophages, this isoform could be the Nox homolog responsible for the increased Nox activity found after ROFA exposure. The

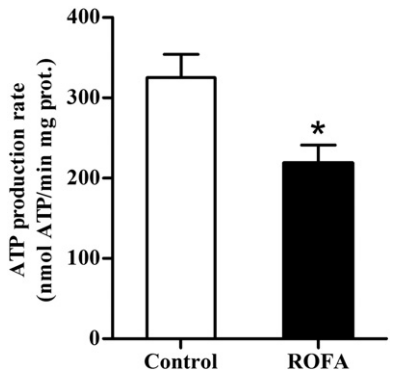

Fig. 3. ATP production rate by lung isolated mitochondria after ROFA exposure. Data is presented as mean ± SEM, n = 6. *$p < 0.05$ vs. control (unpaired *t*-test).

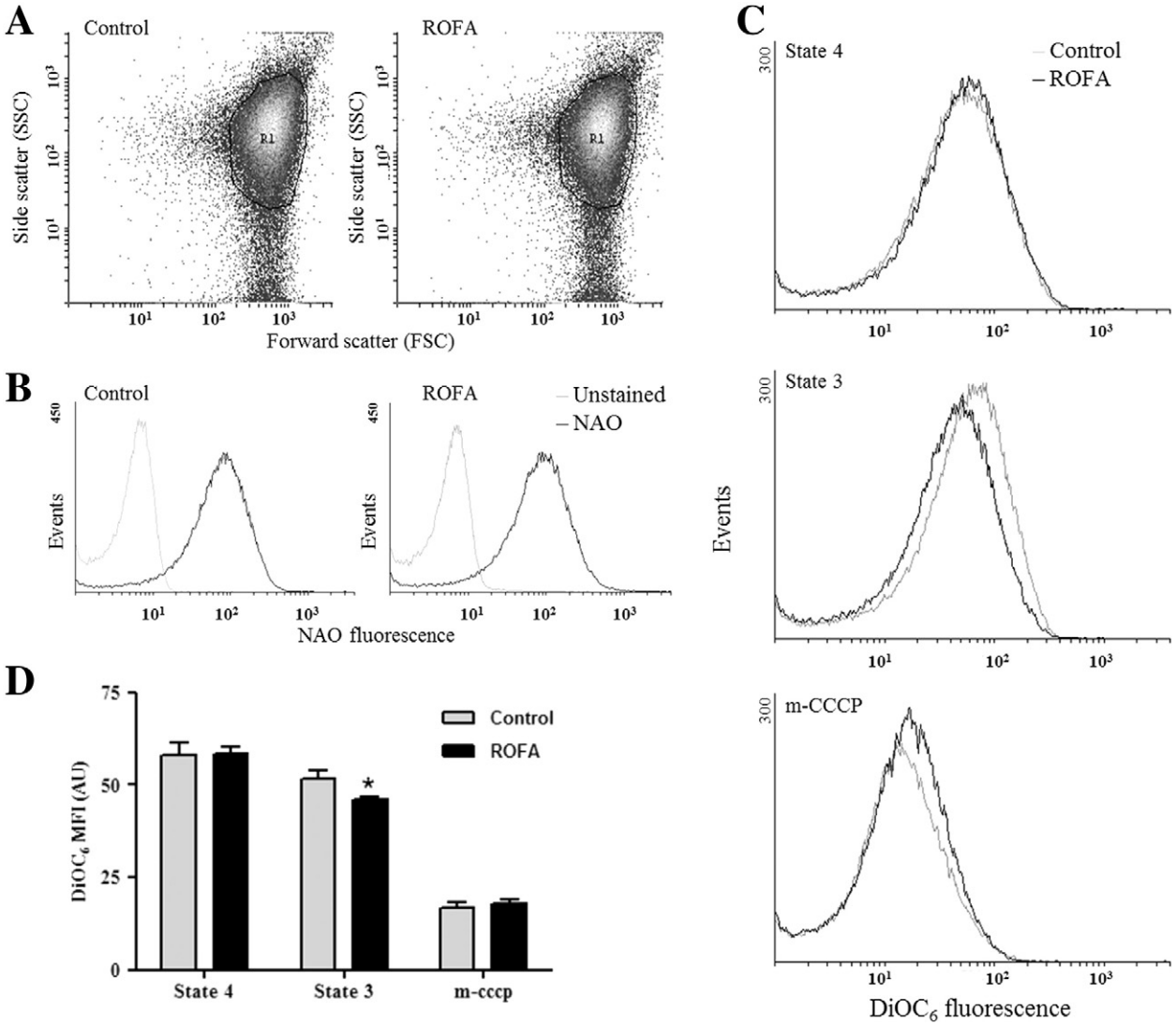

Fig. 4. Mitochondrial membrane potential ($\Delta\Psi_m$) by lung isolated mitochondria after ROFA exposure. (A) Selection of isolated mitochondria from control and ROFA exposed mice based on light scattering properties. (B) Fluorescence of the events in R1 gate for NAO stained mitochondria (black line), compared to an unstained mitochondrial sample (grey line) from control and ROFA-exposed mice. (C) $DiOC_6$ fluorescence from gated mitochondria (R1). Assessment of $\Delta\Psi_m$ was performed in state 4, state 3 and after depolarization with m-CCCP, comparing control and ROFA isolated mitochondria. (D) $DiOC_6$ MFI quantification of state 4, state 3 and after depolarization m-CCCP of control and ROFA isolated mitochondria. Data is presented as mean ± SEM, n = 6. $^*p < 0.05$ vs. state 3 control mitochondria (unpaired *t*-test).

use of gp91 ds-tat as a Nox inhibitor was useful in order to assess the enzymatic activity after ROFA inhalation. Consistently, results obtained for the gp91 ds-tat pretreated group supports the idea that the augmented LCL and NADPH consumption rate was due to Nox activity elicited by ROFA exposure, which may explain the observed increased in tissue O_2 consumption.

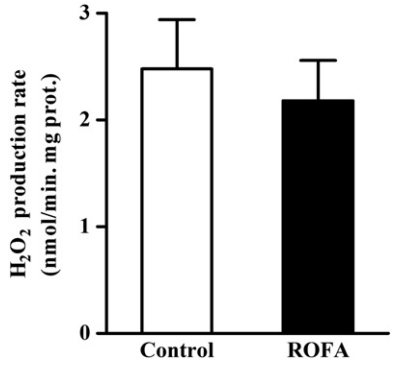

Fig. 5. H_2O_2 production rate by lung isolated mitochondria after exposure to ROFA. Data is presented as mean ± SEM, n = 6.

Once within the tissue, O_2 diffuses to mitochondria where it is reduced by the mitochondrial respiratory chain. The linear rates of O_2 consumption by tissue cubes may be interpreted as a fast oscillation of mitochondria between metabolic state 3 and state 4, driven by either high ATP or ADP levels that decline or stimulate respiration (Boveris and Boveris, 2007). In the present work, exposure to ROFA significantly increased mitochondrial state 3 O_2 consumption, while no significant changes were observed in state 4. No differences between ROFA and control group state 4_O values mean unaltered proton leakiness, showing proper mitochondrial isolation technique (Brand and Nicholls, 2011). Moreover, the uncoupled respiration (state 3_U) showed the same pattern of changes after ROFA inhalation. These changes may indicate that elevated mitochondrial active respiration through a higher complex II activity could contribute to the observed increase in tissue O_2 consumption. This observation was confirmed by the determination of respiratory chain complex activities in mitochondrial membranes, where complex II activity was significantly

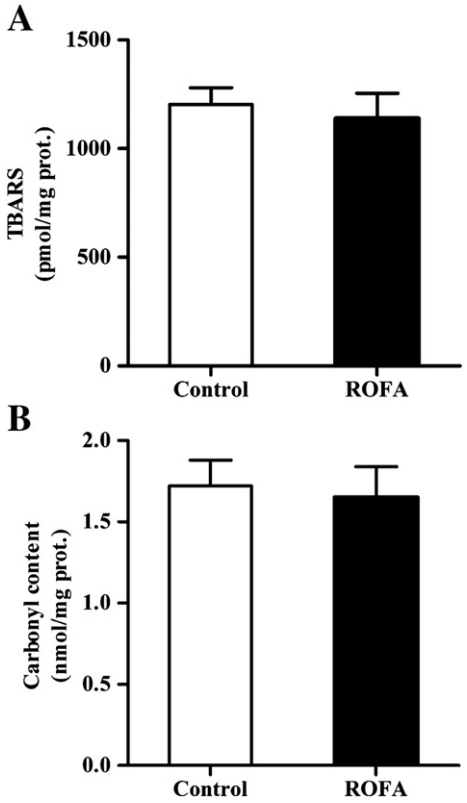

Fig. 6. TBARS levels (A) and carbonyl content (B) in lung isolated mitochondria after exposure to ROFA. Data is presented as mean ± SEM, n = 6.

increased by 25% in ROFA-exposed mice in comparison with the control group. Consistently with our findings, a previous report has shown that in vitro incubation with PM induced mitochondrial dysfunction and increased complex II activity in isolated mitochondria form lung tissue (Delgado-Buenrostro et al., 2012).

Taking into account the data presented in Tables 1 and 2, and in Fig. 2, an analysis of the contribution of the different sources of tissue O_2 consumption rate values can be performed. Our first finding was a 55% increase in O_2 consumption for the ROFA exposed group. When animals exposed to ROFA were pretreated with the Nox inhibitor gp91 ds-tat, a significant 10% increase was still observed, which may account for an increase in mitochondrial respiration (other sources may not be relevant, since the values from animals pretreated with gp91 ds-tat together with the presence of KCN showed no significant differences when compared to the control group). When O_2 consumption rates were assessed in isolated mitochondria, a 34% increase in state 3 was found for ROFA-instilled mice, while no changes were observed in state 4 respiration. In the lung, besides Nox and other O_2-consuming enzymes, the whole tissue O_2 consumption accounts for the sum of the O_2 uptakes of mitochondria respiring in state 3 and of mitochondria respiring in state 4. Under physiological conditions, it can be estimated that the mitochondrial fraction in state 3 is approximately 40% for non-muscular tissues (Boveris and Boveris, 2007). As shown in Table 2, the increase in mitochondrial state 3 respiration may explain the significant 10% increase in animals pretreated with the Nox inhibitor. Furthermore, in order to evaluate the contribution of non-mitochondrial sources to the observed values of lung O_2 consumption, the same measurements were carried out in the presence of KCN. Under these conditions, a significant 27% increase was found in ROFA-exposed mice, which may be attributed to Nox activation since it was abolished in animals pretreated with gp91 ds-tat. Consistently, when Nox activity was estimated with two different experimental approaches, an average 28% increase was found. In conclusion, and in time with the results, the main contributors to the observed increase in lung O_2 consumption appear to be Nox activation, and mitochondrial state 3 respiration increase.

Alterations in mitochondrial function could lead to deficient ATP production. ATP production rate was found to be decreased by 33% in mitochondria isolated from ROFA-exposed mice. These results indicate that ATP supply by oxidative phosphorylation is limited in mice exposed to the ROFA suspension. In addition, lower ATP production leaded to a decreased P/O ratio (number of phosphorylated ADP molecules per oxygen atom, indicative of the oxidative phosphorylation efficiency) therefore, mitochondrial O_2 uptake is not properly converted to chemical energy. Interestingly, a similar effect was observed within heart tissue using the same animal model (Marchini et al., 2012).

Several studies have shown a decreased mitochondrial membrane potential triggered by environmental PM (Di Pietro et al., 2011; Upadhyay et al., 2003). In this case, membrane depolarization was observed during active mitochondrial respiration in ROFA-exposed mice, which could be the responsible for the decreased ATP production rate observed in the ROFA group.

It has been recently shown that mild uncoupling prevents oxidants production by mitochondria, a condition considered to be a highly efficient antioxidant strategy (Alberici et al., 2009). Mild uncoupling is defined by an increased mitochondrial respiratory rate, a decreased in mitochondrial membrane potential, together with a decreased ATP production rate, leading to a low P/O ratio (Cardoso et al., 2010). By increasing electron transport, mitochondria can avoid the oversupply of electron/reducing equivalent into the respiratory chain complexes, known to be substantial $O_2^{\bullet-}$ production sources (Kowaltowski et al., 2009). This view is in agreement with the results shown in the present work, where no significant differences after ROFA exposure were found in mitochondrial H_2O_2 production and the consequent absence of changes in oxidative damage markers to lipids and proteins, as shown through TBARS and carbonyl content values. It has been described that uncoupling proteins and mitochondrial ATP-sensitive channels ($mitoK_{ATP}$) are activated by oxidants. Nox-derived $O_2^{\bullet-}$ may interact with $mitoK_{ATP}$, which could act as a redox sensor (Alberici et al., 2009). Upon the opening of this channel, increased K^+ influx into the matrix could be responsible from the $\Delta\Psi_m$ decrease observed in the ROFA-exposed mice. Inducible H^+ leak has been named as a mechanism for the adjustment of membrane potential to control mitochondrial reactive O_2 species (Mailloux and Harper, 2011).

In conclusion, the present findings show that both Nox activation and mitochondrial respiration are involved in the altered lung O_2 metabolism observed after ROFA inhalation. Nox activation seems to be a relevant non-mitochondrial source of reactive oxygen species in this model. The exposure to ROFA also impacts on mitochondrial function, leading to an increased electron transport rate (evidenced by the higher state 3 respiration), mitochondrial membrane depolarization, decreased ATP production rate and, consequently, deficient oxidative phosphorylation. This situation, known as mild mitochondrial uncoupling, may prevent the mitochondrial generation of reactive O_2 species, which, in turn, could cause oxidative damage within the organelle. The results shown in this work provide new insights in the molecular mechanisms involved in lung injury by O_2 metabolism alterations triggered by PM inhalation.

Funding sources

This study was supported by research grants from the University of Buenos Aires (B413), from Agencia Nacional de Promoción Científica y Tecnológica (PICT 1574), and from Consejo Nacional de Investigaciones Científicas y Técnicas (PIP 358).

Conflict of interest

The authors declare that there are no conflicts of interest.

Acknowledgment

Authors are grateful to Luciano Guerra for the helpful technical assistance on flow cytometry.

References

Aguilera-Aguirre, L., Bacsi, A., Saavedra-Molina, A., Kurosky, A., Sur, S., Boldogh, I., 2009. Mitochondrial dysfunction increases allergic airway inflammation. J. Immunol. 183, 5379–5387.

Alberici, L.C., Oliveira, H.C., Paim, B.A., Mantello, C.C., Augusto, A.C., Zecchin, K.G., Gurgueira, S.A., Kowaltowski, A.J., Vercesi, A.E., 2009. Mitochondrial ATP-sensitive K^+ channels as redox signals to liver mitochondria in response to hypertriglyceridemia. Free Radic. Biol. Med. 47, 1432–1439.

Andreyev, A.Y., Kushnareva, K.E., Starkov, A.A., 2005. Mitochondrial metabolism of reactive oxygen species. Biochemistry 70, 200–214.

Arantes-Costa, F., Lopes, F., Toledo, A., Magliarelli-Filho, P., Moriya, H., Carvalho-Oliveira, R., Mauad, T., Saldiva, P.H., Martins, M., 2008. Effects of Residual Oil Fly Ash (ROFA) in mice with chronic allergic pulmonary inflammation. Toxicol. Pathol. 36, 680–686.

Becker, S., Soukup, J.M., Gallagher, J.E., 2002. Differential particulate air pollution induced oxidant stress in human granulocytes, monocytes and alveolar macrophages. Toxicol. In Vitro 16, 209–218.

Bedard, K., Krause, K.H., 2007. The NOX family of ROS-generating NADPH oxidases: physiology and pathophysiology. Physiol. Rev. 87, 245–313.

Boveris, A., 1984. Determination of the production of superoxide radicals and hydrogen peroxide in mitochondria. Methods Enzymol. 105, 429–435.

Boveris, D.L., Boveris, A., 2007. Oxygen delivery to tissues and mitochondrial respiration. Front. Biosci. 12, 1014–1023.

Boveris, A., Costa, L., Cadenas, E., Poderoso, J., 1999. Regulation of mitochondrial respiration by adenosine diphosphate, oxygen and nitric oxide synthase. Methods Enzymol. 301, 188–198.

Brand, M.D., Nicholls, D.G., 2011. Assessing mitochondrial dysfunction in cells. Biochem. J. 435, 297–312.

Cadenas, E., Boveris, A., 1980. Enhancement of hydrogen peroxide formation by protophores and ionophores in antimycin-supplemented mitochondria. Biochem. J. 188, 31–37.

Cardoso, A.R., Queliconi, B.B., Kowaltowski, A.J., 2010. Mitochondrial ion transport pathways: role in metabolic diseases. Biochim. Biophys. Acta 1797, 832–838.

Chen, L.C., Lippmann, M., 2009. Effects of metal within ambient air particulate matter (PM) on human health. Inhal. Toxicol. 21, 1–31.

Costa, D.L., Dreher, K.L., 1997. Bioavailable transition metals in particulate matter mediate cardiopulmonary injury in healthy and compromised animal models. Environ. Health Perspect. 105, 1053–1060.

Czerniczyniec, A., Karadayian, A.G., Bustamante, J., Cutrera, R.A., Lores-Arnaiz, S., 2011. Paraquat induces behavioral changes and cortical and striatal mitochondrial dysfunction. Free Radic. Biol. Med. 51, 1428–1436.

Delgado-Buenrostro, N.L., Freyre-Fonseca, V., García Cuellar, C.M., Sánchez-Pérez, Y., Gutierrez-Cirlos, E.B., Cabellos-Avelar, T., Orozco-Ibarra, M., Pedraza-Chaverri, J., Chirino, Y.I., 2012. Decreased in respiratory function and electron transport chain induced by airborne particulate matter (PM_{10}) exposure in lung mitochondria. Toxicol. Pathol. http://dx.doi.org/10.1177/01926623312463784.

Di Pietro, A., Visalli, G., Baluce, B., Micale, R.T., La Maestra, S., Spataro, P., De Flora, S., 2011. Multigenerational mitochondrial alterations in pneumocytes exposed to oil fly ash metals. Int. J. Hyg. Environ. Health 214, 138–144.

Dominici, F., Peng, L., Bell, M., Pham, L., McDermott, A., Zeger, S., Samet, J., 2006. Fine particulate air pollution and hospital admission for cardiovascular and respiratory diseases. JAMA 295, 1127–1134.

Drew, B., Leeuwenburgh, C., 2003. Method for measuring ATP production in isolated mitochondria: ATP production in brain and liver mitochondria of Fischer-344 rats with age and caloric restriction. Am. J. Physiol. Regul. Integr. Comp. Physiol. 285, 1259–1267.

Evelson, P., Travacio, M., Repetto, M., Escobar, J., Llesuy, S., Lissi, E., 2001. Evaluation of total reactive antioxidant potential (TRAP) of tissue homogenates and their cytosols. Arch. Biochem. Biophys. 388, 261–266.

Ghio, A., Silbajoris, R., Carson, J., Samet, J., 2002. Biologic effects of oil fly ash. Environ. Health Perspect. 110, 89–94.

Goldsmith, C.A., Imrich, A., Danaee, H., Ning, Y.Y., Kobzik, L., 1998. Analysis of air pollution particulate-mediated oxidant stress in alveolar macrophages. J. Toxicol. Environ. Health A 54, 529–545.

Killingsworth, C.K., Alessandrini, F., Krishna Murty, G.C., Catalano, P.J., Paulauskis, J.D., Godleski, J.J., 1997. Inflammation, chemokine expression, and death in monocrotaline-treated rats following fuel coal ash inhalation. Inhal. Toxicol. 9, 541–545.

Kowaltowski, A.J., de Souza-Pinto, N.C., Castilho, R.F., Vercesi, A.E., 2009. Mitochondria and reactive oxygen species. Free Radic. Biol. Med. 47, 333–343.

Levine, R.L., Williams, J.A., Stadtman, R.E., Shacter, E., 1994. Carbonyl assays for determination of oxidatively modified proteins. Methods Enzymol. 233, 346–357.

Li, N., Xia, T., Nel, A.E., 2008. The role of oxidative stress in ambient particulate matter-induced lung diseases and its implications in the toxicity of engineered nanoparticles. Free Radic. Biol. Med. 44, 1689–1699.

Lowry, O., Rosebrough, A., Farr, A., Randall, R., 1951. Protein measurement with the phenol reagent. J. Biol. Chem. 193, 265–275.

Magnani, N.D., Marchini, T., Tasat, D.R., Alvarez, S., Evelson, P., 2011. Lung oxidative metabolism after exposure to ambient particles. Biochem. Biophys. Res. Commun. 412, 667–672.

Mailloux, R.J., Harper, M.-E., 2011. Uncoupling proteins and the control of mitochondrial reactive oxygen species production. Free Radic. Biol. Med. 51, 1106–1115.

Marchini, T., Magnani, N.D., D'Annunzio, V., Tasat, D.R., Gelpi, R.J., Alvarez, S., Evelson, P., 2012. Impaired cardiac mitochondrial function and contractile reserve following an acute exposure to environmental particulate matter. Biochim. Biophys. Acta 1830 (3), 2545–2552.

Martin, S., Dawidowski, L., Mandalunis, P., Cereceda-Balic, F., Tasat, D.R., 2007. Characterization and biological effect of Buenos Aires urban air particles on mice lungs. Environ. Res. 105, 340–349.

Mela, L., Seitz, S., 1979. Isolation of mitochondria with emphasis on heart mitochondria from small amounts of tissue. Methods Enzymol. 55, 39–46.

Nel, A.E., 2005. Atmosphere. Air pollution-related illness: effects of particles. Science 308, 804–806.

Ostachuk, O., Evelson, P., Martin, S., Dawidowski, L., Yakisich, S., Tasat, D., 2008. Age-related lung cell response to urban Buenos Aires air particle soluble fraction. Environ. Res. 107, 170–177.

Poderoso, J., Fernandez, S., Carreras, M.C., Tchercanski, D., Acevedo, C., Rubio, M., Peralta, J., Boveris, A., 1994. Liver oxygen uptake dependence and mitochondrial function in septic rats. Circ. Shock 44, 175–182.

Pope III, C.A., 2000. Epidemiology of fine particle air pollution and human health: biologic mechanism and who's at risk? Environ. Health Perspect. 108, 713–723.

Rey, F., Cifuentes, M.E., Kiarash, A., Quinn, M.T., Pagano, P.J., 2001. Novel competitive inhibitor of NAD(P)H oxidase assembly attenuates vascular O_2 and systolic blood pressure in mice. Circ. Res. 89, 408–414.

Southam, D.S., Dolovich, M., O'Byrne, P.M., Inman, M.D., 2002. Distribution of intranasal instillations in mice: effects of volume, time, body position, and anaesthesia. Am. J. Physiol. Lung Cell. Mol. Physiol. 282, 833–839.

Upadhyay, D., Panduri, V., Ghio, A., Kamp, D.W., 2003. Particulate matter induces alveolar epithelial cell DNA damage and apoptosis: role of free radicals and the mitochondria. Am. J. Respir. Cell Mol. Biol. 29, 180–187.

Valdez, L.B., Zaobornyj, T., Bombicino, S., Iglesias, D.E., Boveris, A., Donato, M., D'Annunzio, V., Buchholz, B., Gelpi, R.J., 2011. Complex I syndrome in myocardial stunning and the effect of adenosine. Free Radic. Biol. Med. 15, 1203–1212.

van der Vliet, A., 2008. NADPH oxidases in lung biology and pathology: host defences enzymes and more. Free Radic. Biol. Med. 44, 938–955.

van der Vliet, A., 2011. Nox enzymes in allergic airway inflammation. Biochim. Biophys. Acta 1810, 1035–1044.

Vanasco, V., Cimolai, M.C., Evelson, P., Alvarez, S., 2008. The oxidative stress and the mitochondrial dysfunction caused by endotoxemia are prevented by α-lipoic acid. Free Radic. Res. 42, 8.

Vanasco, V., Magnani, N.D., Cimolai, M.C., Valdez, L.B., Evelson, P., Boveris, A., Alvarez, S., 2012. Endotoxemia impairs heart mitochondrial function by decreasing electron transfer, ATP synthesis and ATP content without affecting membrane potential. J. Bioenerg. Biomembr. 44, 243–252.

Vaquero, E.C., Edderkaoui, M., Pandol, S.J., Gukovsky, I., Gukovskaya, A.S., 2004. Reactive oxygen species produced by NAD(P)H oxidase inhibit apoptosis in pancreatic cancer cells. J. Biol. Chem. 279, 34643–34654.

Wei, Y., Sower, J., Nistala, R., Gong, H., Uptergrove, G.M., Clark, S.E., Morris, M.E., Szary, N., Manrique, C., Stump, C., 2006. Angiotensin II-induced NADPH oxidase impairs insulin signaling in skeletal muscle cells. J. Biol. Chem. 281, 35137–35146.

Xia, T., Kovochich, M., Nel, A.E., 2007. Impairment of mitochondrial function by particulate matter (PM) and their toxic components: implications for PM-induced cardiovascular and lung disease. Front. Biosci. 12, 1238–1246.

Yagi, K., 1976. A simple fluorometric assay lipoperoxide in blood plasma. Biochem. Med. 15, 212–216.

Yonetani, T., 1967. Cytochrome oxidase: beef heart. Methods Enzymol. 10, 332–335.